Computational Simulations of DNA Distortions by a *cis,syn*-Cyclobutane Thymine Dimer Lesion†

Karol Miaskiewicz,*,‡ John Miller,‡ Michael Cooney,‡ and Roman Osman§

Contribution from the Pacific Northwest National Laboratory, Richland, Washington 99352, and Department of Physiology and Biophysics, Mount Sinai School of Medicine of the City University of New York, New York, New York 10029

Received April 5, 1996. Revised Manuscript Received July 24, 1996⊗

Abstract: Results are presented from 500 ps molecular dynamics simulations on the native dodecamer d(CGC-GAATTCGCG)$_2$ and the lesioned dodecamer containing a *cis,syn*-thymine cyclobutane dimer at the TT step. The computations, performed with AMBER4.1, included explicitly represented solvent with periodic boundary conditions applied within the constant temperature and pressure algorithm. Electrostatic interactions were calculated with the particle-mesh Ewald method. Distortions to DNA structure produced by the lesion were found to be localized at the dimer site and include mainly a substantial kink in the helical axis, rolled and tilted base pairs, and weakened hydrogen bonding at the 5′ base pair of the lesion. A slight change in orientation around the glycosyl bond for the 5′ thymine of the lesion and highly stiffened deoxyribose rings for both thymine bases were also observed. The global curvature of DNA is increased by about 10° by dimer incorporation. Calculations of H(1′)-H(6)(pyrimidine) and H(1′)-H(8)-(purine) interproton distances from the performed simulations agree very well with the pattern of NMR NOE signals reported in various dimer containing oligonucleotides, where an interruption of NOE connectivities is found on the 5′ side of the lesion. Comparison of the pattern of distortions observed at the dimer site with the crystal structure of a complex between dimer-containing DNA and repair enzyme endonuclease V (*Cell* **1995**, *83*, 773−782) leads to the hypothesis that dimer recognition may involve a whole pattern of small distortion at the lesion site rather than one particular structural/dynamical feature associated with the lesion.

Introduction

The correlation observed between sunlight exposure and skin cancer underscores the biological importance of UV-induced damage to DNA. Cyclobutane pyrimidine dimers together with (6-4) photoadducts of pyrimidines are the major products formed in DNA upon exposure to UV radiation (reviewed in ref 1). Mutations caused by the absorption of UV radiation occur predominantly at dipyrimidine sequences; hence, they are usually attributed to the presence of pyrimidine cyclobutane dimers and/or 6,4-photoproducts.[2] The mutagenicity of these lesions is frequently explained by miscoding during DNA replication due to perturbations of base-pairing interactions; however, the mutagenicity of UV photoproducts depends of their sequence context,[3] so that more global structural changes than base-pairing ability probably contribute to mutation induction.

Repair of DNA containing cyclobutane pyrimidine dimers can occur by several different enzymatic pathways. DNA photolyases (reviewed in ref 4) catalyze photocleavage of the CC bonds linking adjacent C(5) and C(6) atoms in the dimer, thereby restoring the pyrimidines to their native state. Pyrimidine dimers may also be removed by the nucleotide-excision repair pathway.[5,6] In this type of repair the damaged bases are removed from DNA as an oligonucleotide and the resulting gap is filled by repair synthesis.

Cyclobutane pyrimidine dimers are also removed by the base-excision pathway. The most extensively studied enzyme of this type is bacteriophage T4 endonuclease V. This enzyme has a glycosylase activity that hydrolyses the glycosyl bond of the 5′ pyrimidine in the dimer and an apurinic/apyrimidinic endonuclease activity proceeding through the β-elimination of the 3′-phosphate of an abasic site.[7] The high resolution X-ray crystal structure of endo V[8] combined with numerous site-directed mutagenesis studies[7,9] have allowed the most important residues for binding and catalytic activities to be identified. Recently, an X-ray crystal structure of endonuclease V complexed with duplex DNA containing a thymine dimer was reported.[10] Substantial distortions to DNA structure were observed in the complex including an extra-helical adenine base complementary

† Abbreviations: MD, molecular dynamics; PME, particle mesh Ewald method; NMR, nuclear magnetic resonance; NOE, nuclear overhauser effect; NOESY, nuclear overhauser effect spectroscopy; RMSD, root mean square deviation; ESP, electrostatic potential.

‡ Pacific Northwest National Laboratory.

§ Mount Sinai School of Medicine of the City University of New York.

* Author to whom correspondence should be addressed to: DASGroup, Inc., P.O. Box 5428, Johnstown, PA 15904.

⊗ Abstract published in *Advance ACS Abstracts*, September 1, 1996.

(1) Cadet, J.; Vigny, P. *Bioorganic Photochemistry*; H. Morrison, Ed.; John Wiley & Sons: New York, 1990; Vol. 1, pp 1−272.

(2) Hutchinson, F. *Photochem. Photobiol.* **1987**, *45*, 897−903.

(3) Brash, D. E.; Seetharam, S.; Kraemer, K. H.; Seidman, M. M.; Bredberg, A. *Proc. Natl. Acad. Sci. U.S.A.* **1987**, *84*, 3782−3786.

(4) Sancar, G. B. *Mutat. Res.* **1990**, *236*, 147−160.

(5) Sancar, A.; Sancar, G. B. *Ann. Rev. Biochem.* **1988**, *57*, 29−67.

(6) Van Houten, B.; Snowden, A. *BioEssays* **1993**, *15*, 1−9.

(7) Schrock, R. D., III; Lloyd, R. S. *J. Biol. Chem.* **1991**, *266*, 17631−17639.

(8) Morikawa, K.; Matsumoto, O.; Tsujimoto, M.; Katayanagi, K.; Ariyoshi, M.; Doi, T.; Ikehara, M.; Inaoka, T.; Ohtsuka, E. *Science* **1992**, *256*, 523−526.

(9) Augustine, M. L.; Hamilton, R. W.; Dodson, M. L.; Lloyd, R. S. *Biochemistry* **1991**, *30*, 8052−8059. Dodson, M. L.; Prince, M. A.; Anderson, W. F.; Lloyd, R. S. *Mutat. Res.* **1991**, *255*, 19−29. Dodson, M. L.; Schrock, R. D. III.; Lloyd, R. S. *Biochemistry* **1993**, *32*, 8284−90. Doi, T.; Recktenwald, A.; Karaki, Y.; Kikuchi, M.; Morikawa, K.; Ikehara, M.; Inaoka, T.; Hori, N.; Ohtsuka, E. *Proc. Natl. Acad. Sci. U.S.A* **1992**, *89*, 9420−9424. Dowd, D. R.; Lloyd, R. S. *Biochemistry* **1989**, *28*, 8699−8705. Nickell, C.; Lloyd, R. S. *Biochemistry* **1991**, *30*, 8638−8648. Prince, M. A.; Friedman, B.; Gruskin, E. A.; Schrock, R. D. III.; Lloyd, R. S. *J. Biol. Chem.* **1991**, *266*, 10686−93. Recinos, A.; Lloyd, R. S. *Biochemistry* **1988**, *27*, 1832−1838. Schrock, R. D. III; Lloyd, R. S. *J. Biol. Chem.* **1993**, *268*, 880−886. Stump, D. G.; Lloyd, R. S. *Biochemistry* **1988**, *27*, 1839−1843. Ishida, M.; Kanamori, Y.; Hori, N.; Inaoka, T.; Ohtsuka, E. *Biochemistry* **1990**, *29*, 3817−3821.

(10) Vassylyev, D. G.; Kashiwagi, T.; Mikami, Y.; Ariyoshi, M.; Iwai, S.; Ohtsuka, E.; Morikawa, K. *Cell* **1995**, *83*, 773−782.

S0002-7863(96)01130-4 CCC: $12.00

to 5′ thymine of the dimer and a sharp helical kink at the dimer position. Even with the insights provided by these new experimental data, the major structural/energetical factors recognized by the enzyme are still not clear.

Detailed information on the perturbations to DNA structure caused by pyrimidine dimers is crucial to understanding the mechanisms of enzymatic recognition of this lesion. However, the available experimental results are not only incomplete, they are also often contradictory. Results from gel electrophoresis studies were interpreted as evidence for a bend of about 30° in the helical structure due to the presence of a thymine dimer.[11] However, more recent gel electrophoresis experiments with a DNA 21-mer found the dimer inducing a bend of only ≈7°.[12] A similar, small bend of only about 9° was determined by NMR in a dimer containing decamer.[13] In general, NMR studies performed on DNA oligonucleotides containing a *cis,syn*-pyrimidine dimer showed that the distortions caused by the lesion are surprisingly small and localized to the immediate vicinity of the dimer.[13−18] Similar conclusions were drawn by Barone et al.[19] based on thermal denaturation, hydroxyl radical footprinting, and optical experiments on a 21-base-pair oligonucleotide containing a single thymine dimer. Thermodynamic parameters determined by their work showed that the presence of a dimer does not significantly change stacking or hydrogen bond interactions in the 21mer; however, small distortions of an unspecified nature were postulated on the 5′ side of the lesion.[19] In contrast, small perturbations in NMR spectral parameters have been observed in the vicinity of the lesion on the 3′ side.[17,18]

Two computational studies based on molecular mechanics came to quite different conclusions regarding the effects of a *cis,syn*-cyclobutane thymine dimer on the same DNA sequence.[20,21] One of these studies predicted extensive bending and kinking, while in the other, these effects were not detected at all. Since structural optimization in molecular mechanics converges to the closest minimum of the potential energy, this discrepancy might be due to differences in the starting geometries. A molecular dynamics study on the dimer containing dodecamer was also reported,[22] which found a substantial degree of kinking. However, this study used rather simplistic models of solvent and electrostatic interactions.

Early molecular dynamics (MD) simulations of nucleic acids that used a cutoff distance to truncate electrostatic interactions displayed extensive distortions to DNA structure[23] which, in some cases, were controlled by the introduction of artificial restraints.[24] However, substantial progress has been made recently in the quality of MD simulations for nucleic acids due to a very efficient implementation of reciprocal space Ewald sums by the particle mesh Ewald (PME) method.[25] The utility of the PME method was clearly demonstrated by reports on successful simulations of nucleic acids both in crystals and aqueous solutions.[26,27] In these cases, the structures of nucleic acids in PME simulations remained very close to the initial crystallographic or canonical conformations. Recently, long PME simulations (≈1 ns) of a DNA decamer were shown to converge to the same conformation, which was consistent with experimental data, even starting from structures as different as canonical A- and B-DNA.[28] This indicates that the PME method does not introduce artificial stability around a starting structure.

Table 1. Average Distance between H(1′) and H(6) (Pyrimidine) or H(8) (Purine) on the 3′ Adjacent Base during the 300−500 ps Time Period of Molecular Dynamics Simulation

damaged strand		nondamaged strand	
residues	distance (Å)	residues	distance (Å)
C1/G2	4.0	C13/G14	3.1
G2/C3	3.7	G14/C15	3.6
C3/G4	4.2	C15/G16	3.9
G4/A5	4.1	G16/A17	4.0
A5/A6	3.9	A17/A18	4.1
A6/T7	5.9	A18/T19	4.3
T7/T8	4.4	T19/T20	4.1
T8/C9	4.6	T20/C21	4.4
C9/G10	3.9	C21/G22	4.6
G10/C11	4.0	G22/C23	3.8
C11/G12	5.0	C23/G24	4.1

This paper presents the results of a 500 ps PME simulation on the dodecamer d(CGCGAATTCGCG)$_2$ with and without a *cis,syn*-cyclobutane thymine dimer. The new force-field parametrization for nucleic acids by Cornell et al.[29] is used along with explicit representation of water and counterions. Whereas previous simulations (with cutoff truncated electrostatic interactions) of damaged oligonucleotides have provided rather promising results,[30] the capability of MD method to succesfully describe perturbations to DNA caused by lesions is not fully established. The simulations presented here are, to our knowledge, the first published study on lesioned/modified DNA oligonucleotide using MD method with PME approach. General agreement with available experimental structural results observed in present work suggests that the applied computational model is accurate. However, it should be kept in mind that more studies on damaged DNA sequences, both experimental and computational, are desired for full validation of this theoretical model in DNA damage studies.

(11) Husain, I.; Griffith, J.; Sancar, A. *Proc. Natl. Acad. Sci. U.S.A.* **1988**, *85*, 2558−2562.
(12) Wang, C. -I.; Taylor, J. -S. *Proc. Natl. Acad. Sci. U.S.A.* **1991**, *88*, 9072−9076.
(13) Kim, J.-K.; Patel, D.; Choi, B.-S. *Photochem. Photobiol.* **1995**, *62*, 44−50.
(14) Kemmink, J.; Boelens, R.; Koning, T.; van der Marel, G. A.; van Boom, J. H.; Kaptein, R. *Nucleic Acids Res* **1987**, *15*, 4645−4653.
(15) Kemmink, J.; Boelens, R.; Kaptein, R. *Eur. Biophys. J.* **1987**, *14*, 293−299.
(16) Kemmink, J.; Boelens, R.; Koning, T.; Kaptein, R.; van der Marel, G. A.; van Boom, J. H. *Eur. J. Biochem.* **1987**, *162*, 37−43.
(17) Taylor, J.-S.; Garrett, D. S.; Brockie, I. R.; Svoboda, D. L.; Telser, J. *Biochemistry* **1990**, *29*, 8858−8866.
(18) Lee, B. J.; Sakashita, H.; Ohkubo, T.; Ikehara, M.; Doi, T.; Morikawa, K.; Kyogoku, Y.; Osafune, T.; Iwai, S.; Ohtsuka, E. *Biochemistry* **1994**, *33*, 57−64.
(19) Barone, F.; Bonincontro, A.; Mazzei, F.; Minoprio, A.; Pedone, F. *Photochem. Photobiol.* **1995**, 61, 61−67.
(20) Rao, S. N.; Keppers, J. W.; Kollman, P. *Nucleic Acids Res.* **1984**, *12*, 4789−4807.
(21) Pearlman, D. A.; Holbrook, S. R.; Pirkle, D. H.; Kim, S.-H. *Science* **1985**, *227*, 1304−1308.
(22) Rao, S. N.; Kollman, P. A. *Bull. Chem. Soc. Jpn.* **1993**, *66*, 3133−3134.
(23) Miaskiewicz, K.; Osman, R.; Weinstein, H. *J. Am. Chem. Soc.* **1993**, *115*, 1526−1537.
(24) Swaminathan, S.; Ravishanker, G.; Beveridge, D. L. *J. Am. Chem. Soc.* **1991**, *113*, 5027−5040.
(25) Darden, T.; York, D.; Pedersen, L. *J. Chem. Phys.* **1993**, *98*, 10089−10092.
(26) York, D. M.; Yang, W.; Lee, H.; Darden, T.; Pedersen, L. G. *J. Am. Chem. Soc.* **1995**, *117*, 5001−5002. Lee, H.; Darden, T. A.; Pedersen, L. G. *J. Chem. Phys.* **1995**, *102*, 3830−3834. Weerasinghe, S.; Smith, P. E.; Mohan, V.; Cheng, Y. -K.; Pettitt, B. M. *J. Am. Chem. Soc.* **1995**, *117*, 2147−2158.
(27) Cheatham, III, T. E.; Miller, J. L.; Fox, T.; Darden, T. A.; Kollman, P. A. *J. Am. Chem. Soc.* **1995**, *117*, 4193−4194.
(28) Cheatham, III, T. E.; Kollman, P. A. *J. Mol. Biol.* **1996**, *259*, 434−444.
(29) Cornell, W. D.; Cieplak, P.; Bayly, C. I.; Gould, I. R.; Merz, K. M.; Ferguson, D. M.; Spellmeyer, D. C.; Fox, T.; Caldwell, J. W.; Kollman, P. A. *J. Am. Chem. Soc.* **1995**, *117*, 5179−5197.
(30) Miaskiewicz, K.; Miller, J.; Ornstein, R.; Osman, R. *Biopolymers* **1994**, *35*, 113−124.

The present study shows that structural distortion to DNA induced by the lesion are highly localized and include perturbations in base pairing and stacking mostly on the 5′ side of the dimer. In general, the lesioned dodecamer remains in B-DNA geometry with additional bending by about 10° relative to the native sequence. This good agreement with the available experimental data indicates that our results can provide a basis for studies of recognition and repair of this important DNA lesion.

Methods

A *cis*,*syn*-cyclobutane thymine dimer was incorporated into the double-helical dodecamer d(CGCGAATTCGCG)$_2$ with a canonical B-DNA initial geometry. The thymine dimer was formed inside DNA during preliminary energy minimizations on the hydrated dodecamer. First, the positions of counterions and water were optimized with the DNA fixed in the canonical B conformation. This was followed by two steps of minimization of the whole system but without the C(5)−C(5) and C(6)−C(6) bonds between the adjacent thymine bases of the dimer. Instead of defining these bonds in the topology file, which would result in large forces from the harmonic potential approximation, restraints on the atom−atom distances were applied; $R = 3$ and 2 Å in the first and second steps of minimization, respectively. A force constant of 100 kcal/mol was used in both step. All the restraints were removed in the final stage of minimization, and the covalent bonds C(5)−C(5) and C(6)−C(6) were formed. In a procedure similar to that used by Rao et al.,[20] C(5) and C(6) of the thymines engaged in dimer formation were changed from CM to CT atom type (i.e., from sp^2 to sp^3 hybridization). STO-3G calculations were performed on native thymine and the *cis*,*syn*-cyclobutane thymine dimer with methyl groups at the N(1) positions simulating the C(1′) atom of deoxyribose and atomic charges were obtained by fitting to the electrostatic potential. Changes in thymine charges due to dimer formation were negligible except in the following cases: N(1) (−0.0206), C(6) (−0.0133), H(6) (−0.0207), C(5) (0.0602), and C(7) (−0.0056), where the number in parentheses is the charge in the dimer minus the charge on native thymine. These charge increments, which sum to zero, were added to the standard AMBER 4.1 atomic charges for the thymine bases involved in dimer formation. Since dimer formation has little effect on thymine charges, these STO-3G charge increments should be adequate, even though most of the atomic charges in the AMBER 4.1 force field were obtained by ESP fitting with HF/6-31G* wave functions.[29]

The dodecamer structure, modified to include a thymine dimer by the above procedure, was used to setup a PME molecular dynamics simulation. To neutralize negative charges on phosphates, 22 Na^+ ions were placed around phosphate groups, then the DNA molecule and its counterions were placed in a rectangular box of TIP3P water with dimensions 68/44/44 Å. The complete system of DNA, water, and counterions contained 12 600 atoms. Minimization and equilibration/heating of the system followed the procedure described by Cheatham et al.[27] After equilibration, a 500 ps production run was performed. The constant pressure and constant temperature algorithm of AMBER 4.1[31] was used with the SHAKE constraint on bonds with hydrogen atoms and a 0.002 ps time step. Electrostatic forces were calculated by the PME method as implemented in AMBER 4.1 and a cutoff distance of 9 Å was used for Lennard-Jones interactions. Structures generated during the simulation were analyzed using the program CURVES[32,33] applied as a standalone version and as implemented within the DIALS_AND_WINDOWS program.[34]

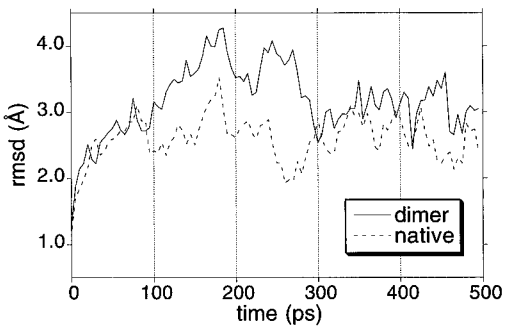

Figure 1. Comparison of RMSD positional deviations of heavy atoms from their positions in the minimized starting structures during the simulations of the native and lesioned dodecamers.

Results

Figure 1 shows root mean square deviations (RMSD) of heavy atoms from their positions in the respective minimized starting structures during MD simulations performed on the dodecamer d(CGCGAATTCGCG)$_2$ with and without a *cis*,*syn*-cyclobutane dimer at the T7-T8 position. Although the native sequence displays conformational equilibrium after 100 ps of simulation, the RMSD plot for the modified dodecamer shows a plateau only after 300 ps. Therefore, only conformations generated during the 300−500 ps period of both simulations were used to calculate averaged structural properties. The equilibrated structure of the native sequence has an RMSD of about 2.5 Å away from the starting B-DNA conformation, which is significantly less than found in earlier simulations using AMBER4.0 and a cutoff distance to truncate electrostatic interactions.[23] The lesioned sequence exhibits RMSD values only slightly higher in the 300−500 ps period than those observed for the native dodecamer. Thus, both sequences remain very close to canonical B-DNA form during the course of performed simulations.

Axis-base-pair parameters, that describe the location and orientation of base pairs relative to the helical axis, are shown in Figure 2 for the lesioned sequence. **X-displacement** (**XDP**) and **inclination** (**INC**) are the two principal diagnostic parameters that differentiate the A and B forms of DNA. The structure of the lesioned dodecamer exhibits values of both **XDP** and **INC** that are very close to those characteristic of B-DNA. Similar behavior is also observed in the native sequence (results not shown). The **tip angle** (**TIP**) shows an abrupt change at position T7-A18, which indicates a site of bending of helical axis that is not observed in the native sequence.

Global DNA curvature was calculated by fitting a circle to the set of helical axis reference points determined by CURVES.[35] The magnitude of curvature is calculated as an angle formed by the two radii that encompass the DNA axis (Figure 3). In addition, the direction of global curvature was determined by taking the angle between the projections of two vectors on the mean plane of the central A6-T19 base pair. One of these vectors is a vector from the point on the fitted circle for the A6-T19 base pair to the center of the circle. The other is the dyad axis vector for A6-T19, defined as the vector connecting

(31) Pearlman, D. A.; Case, D. A.; Caldwell, J. W.; Ross, W. S.; Cheatham III, T. E.; Ferguson, D. M.; Seibel, G. L.; Singh, U. C.; Weiner, P. K.; Kollman, P. A. AMBER 4.1; University of California: San Francisco, 1995.

(32) Lavery, R.; Sklenar, H. *J. Biomol. Struct. Dyn.* **1988**, *6*, 63−91.

(33) Lavery, R.; Sklenar, H. *J. Biomol. Struct. Dyn.* **1988**, *6*, 655−667.

(34) Ravishanker, G.; Swaminatham, S.; Beveridge, D. L.; Lavery, R.; Sklenar, H. *J. Biomol. Struct. Dyn.* **1989**, *6*, 669−699.

(35) Norberto de Souza, O. Ph.D. Thesis, University of London, 1994.

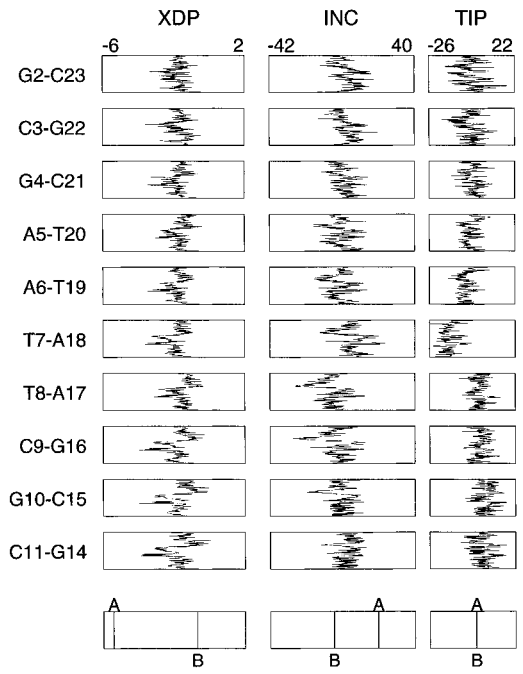

Figure 2. Base pair-helical axis parameters: Xdisplacement (XDP), inclination (INC), and tip (TIP) describe the position and orientation of base pairs relative to the helical axis in the lesioned dodecamer. Time of the simulation increases from 0 to 500 ps from the bottom to the top of the window. The range of variation in the parameter is indicated on the top window in each column, and its value in canonical A- and B-DNA is shown in the bottom row of windows. The end base pairs have been omitted from the plot.

the midpoint of the C(1′) atoms to the midpoint of purine C(6) and pyrimidine C(8) atoms. The assigned directions of these two vectors are such, that an angle of 0° between them means a bend toward the major groove (i.e., compressing the major groove), while 180° means a bend toward the minor groove. It should be noted, that the above method of curvature calculation is size dependent and thus results can be compared only for equal length sequences.

Global DNA curvature, analyzed with the above method, is illustrated in Figure 3. Very good fits of a circle/arc to the helical axis were obtained in this study (as well as for other sequences that we have analyzed with this method so far); hence, the description of DNA (or rather DNA axis) as arc shaped is quite accurate. Although calculated magnitudes of curvature exhibited considerable variation during the simulations, a statistically significant shift in its distribution toward larger values is observed when the dimer lesion is present. The average curvature magnitude increased by 11° from a value of 28° for the native sequence to a value of 39° for the lesioned dodecamer. The direction of curvature is toward the major groove in both cases. However, the direction of curvature fluctuates substantially less in the dimer containing sequence. When increased magnitude of global curvature is combined with decreased fluctuations in its directionality, the dimer lesion shows a rather significant effect on enhancing DNA's global curvature.

Two methods were applied to analyze the DNA curvature on the local level. The circle/arc fitting method used for calculating global curvature was applied to small segments of helical axis containing just three base-pairs (Figure 4A). In addition, the angle between local segments of helical axis obtained from CURVES was analyzed (Figure 4B). For the native sequence, both methods identified kinks located at the C3/G4 and C9/G10 steps. Similar locations of bends/kinks were found in the crystal structure of d(CGCGAATTCGCG)$_2$ when analyzed with the CURVES algorithm.[32] The two kinks seen in the native dodecamer are also observed in the lesioned sequence, although they appear to be attenuated. In addition, the lesioned sequence displays a large bending/kink located at the T7/T8 step, i.e., at the dimer position. This extra kink causes the lesioned DNA to have greater overall curvature than the native one, in spite of the reduction in magnitude of the other two kinks when the dimer is present. An angle between helical axis elements has two components in the CURVES analysis:[33] axis inclination and axis tip. In our sequences, the overall axis angles are determined by the dominant contributions from axis tip angles (data not shown), which are positive at every dinucleotide step, thus, indicating that all local bends/kinks observed in studied sequences are toward the major groove (i.e., compressing the major groove).

Backbone torsional angles of both dodecamers (Figure 5) remain in the regions expected for right-handed DNA structures. Simultaneous transitions of ϵ and ζ torsional angles are seen at C3, A5, and C9 in the native sequence and at C3 and A5 in the lesioned one. The so-called "crankshaft" transitions of α and γ torsional angles seen in early simulations[23,24,36] with cutoff truncated electrostatic interactions were not observed here. The thymine dimer does not change the pattern of backbone angles in a significant way. The only changes that can be clearly attributed to the presence of the lesion were in the glycosyl bond dihedral χ at T7 (the 5′ thymine of the dimer), which shows *syn* conformation instead of *anti* conformation observed at the other bases in the dodecamer, and the deoxyribose puckering phase angles ϕ of T7 and T8. Most deoxyribose rings are very flexible in the performed simulations: values of ϕ cover the whole range between the ^{3}E and ^{2}E conformations characteristic for A-DNA and B-DNA, respectively. However, at the dimer site the deoxyribose rings are significantly more rigid (Figure 5), with B-DNA like puckering prevailing at the 5′ thymine and more A-DNA type puckering favored at the 3′ thymine of the dimer.

The localized effects of the thymine dimer on DNA geometry are clearly seen in the base-pairing interactions. *Intrabase pair* parameters in Figure 6 illustrate base-pairing geometries in the lesioned dodecamer. Significant changes in **buckle** (**BKL**) and **propeller twist** (**PRP**) occurs at the T7-A18 base pair. The other base pair involved in the lesion (i.e., T8-A17) shows essentially the same base-pairing geometry as that observed at nonlesioned positions of the damaged dodecamer and in the native dodecamer (results not shown).

Distortions of base-pairing parameters observed for T7-A18 base pair are reflected in the parameters of Watson−Crick hydrogen bonds at this position (Figure 7). The N(1)···H(3)-N(3) hydrogen bond of T7-A18 is stretched by about 0.5 Å, and the hydrogen bond angle is only about 125°; both suggesting a weakening of this bond. The other hydrogen bond in the T7-A18 base pair as well as both hydrogen bonds at the T8-A17 base pair do not show significant distortion.

Significant distortions are also observed for the *interbase pair* parameters (Figure 8) that describe the geometry of base stacking in the lesioned sequence. These distortions are observed at the A6-T19/T7-A18 and the T7-A18/T8-A17 steps. At the A6-T19/T7-A18 step **tilt** (**TLT**) becomes more positive and **roll** (**ROL**) is slightly more negative than at the other steps. At the T7-A18/T8-A17 steps, shifts in the opposite direction are observed, i.e., more negative **tilt** and significantly increased

(36) Srinivasan, J.; Withka, J. W.; Beveridge, D. L. *Biophys. J.* **1990**, *58*, 533−548.

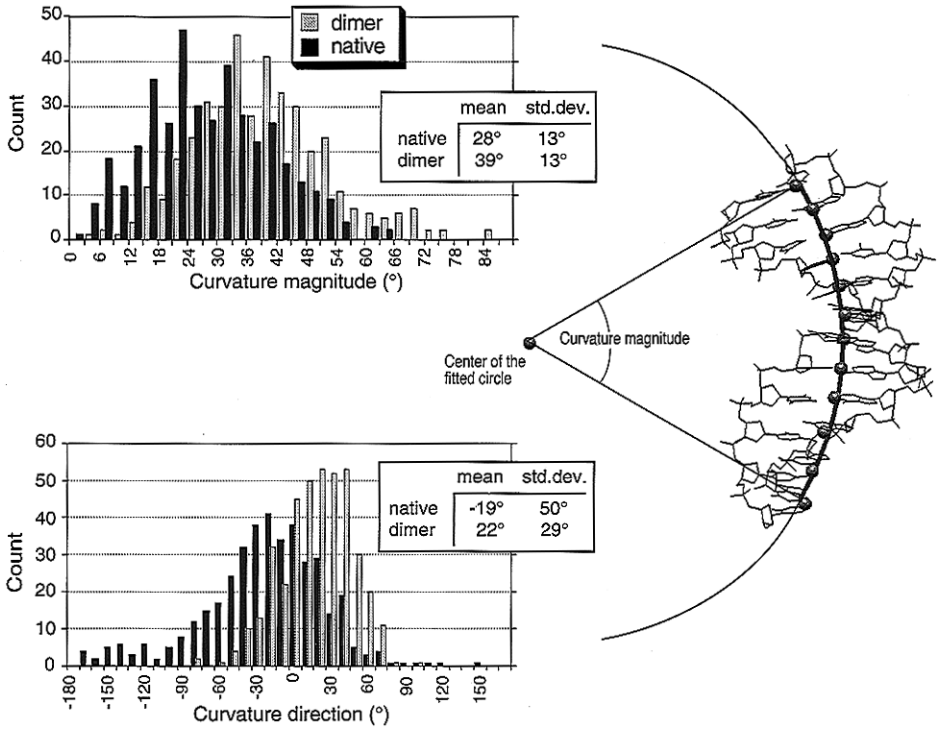

Figure 3. Global curvature of DNA analyzed by fitting a circle/arc to the helical axis points (shown by balls). Distribution of calculated magnitude of curvature and its direction (see text) in the native and lesioned dodecamers is shown (300−500 ps time period of simulations).

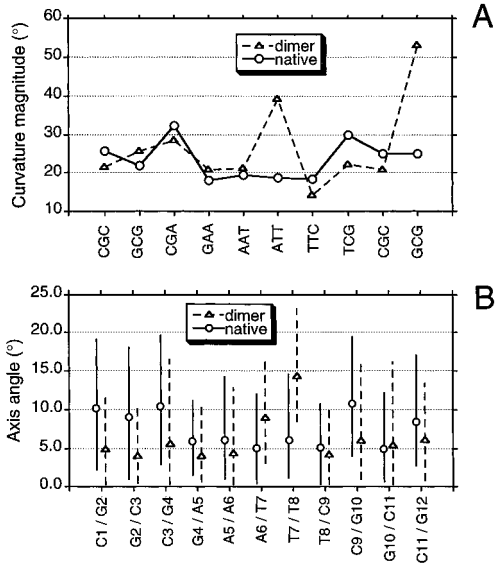

Figure 4. A. Magnitude of curvature calculated for three base-pair elements of the helical axis by the circle fitting method. B. An angle between local segments of helical axis obtained from CURVES analysis.[32,33] Vertical bars indicate a range of values observed at base-pair steps with a mean value indicated by a marker. Both plots prepared for the 300−500 ps time period of simulations.

(more positive) **roll**. In addition, helical **twist** (**TWS**) is decreased slightly at the T7-A18/T8-A17 step.

Discussion

Despite many experimental and theoretical studies, the mechanism by which repair enzymes recognize pyrimidine dimers is still elusive, mainly due to lack of detailed information on the perturbations to DNA structure and dynamics caused by pyrimidine dimers. In this work, structural distortions in a DNA dodecamer containing a thymine dimer were analyzed by computational methods.

Probably the main controversy about pyrimidine dimers concerns their effect on global DNA curvature. Our calculations indicate that dimer incorporation introduces a visible kink/bend of about 15° at the dimer location. Global curvature of the dodecamer is affected only slightly by this kink with overall bend increasing from 28° to 39°. The sequence chosen for this study had naturally occurring kinks on both sides of the dimer. Formation of a kink at the dimer location decreases the magnitude of the other two kinks, which may explain the small effect of the dimer on global curvature. This explanation implies that the effect of a thymine dimer on global curvature will depend on its sequence context. Interestingly, the sharp kink of about 60° was observed at the dimer location in the complex formed between lesioned DNA and repair enzyme endonuclease V.[10] Our calculations suggest that endonuclease V may recognize and enhance a pre-existing kink of smaller magnitude in the lesioned DNA.

The *cis*,*syn*-thymine dimer does not appear to have a significant effect on DNA backbone conformation. The only distortions in the backbone that can be extracted from our calculations concern the conformation about the glycosyl bond and the sugar puckering. Whereas the glycosyl bond torsional angle χ at the 3′ thymine of the dimer remains in the *anti* conformation around −120°, as at other bases of the dodecamer, the 5′ thymine of the lesion shows χ substantially increased to about −60° (*high-anti*). This result is in agreement with NMR data obtained on an octamer containing a thymine dimer, where an increase in the glycosyl torsion angle was observed only at the 5′ thymine.[16] However, it should also be mentioned here that perturbations in χ at both bases were postulated from NMR spectra of d(TpT) containing the dimer.[37]

The deoxyribose rings of both thymine bases involved in cyclobutane linkage formation are substantially more rigid than at other positions in the sequence. Although the deoxyribose ring of the 5′ thymine remains near the ^{2}E conformation, ring conformation at the 3′ thymine is in the ^{O}E range (O1′-endo),

(37) Hruska, F. E.; Wood, D. J.; Ogilvie, K. K.; Charlton, J. L. *Can. J. Chem.* **1975**, *53*, 1193−1203.

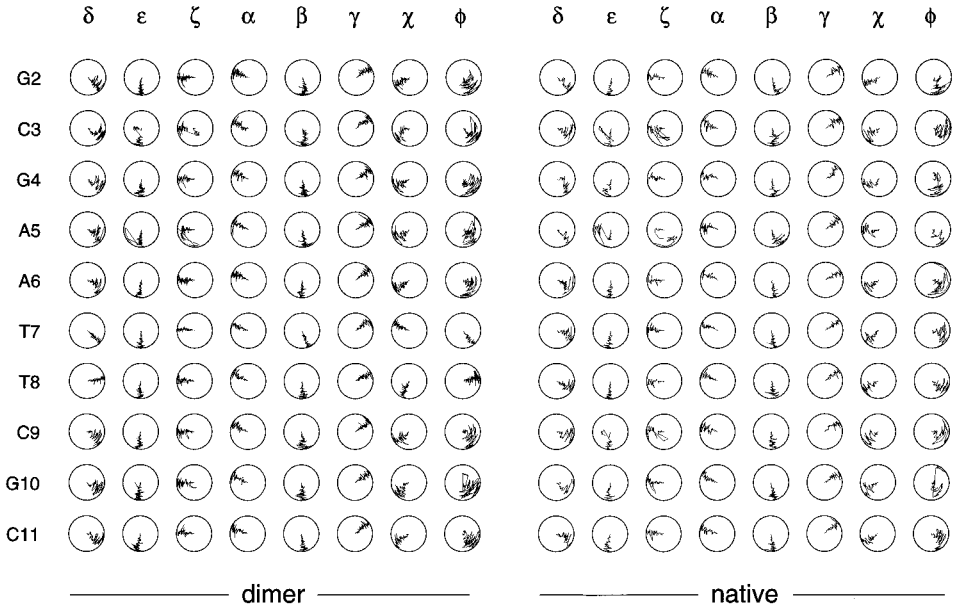

Figure 5. Dials for backbone torsional angles in the damaged strand in the lesioned sequence and respective strand in the native dodecamer. Time increases from 0 to 500 ps between the center and circumference of the dials. The 0°/360° value is at the top of a dial (12:00 h), and the 180° is at the bottom of the dial (6:00 h). The end bases are omitted from the plot.

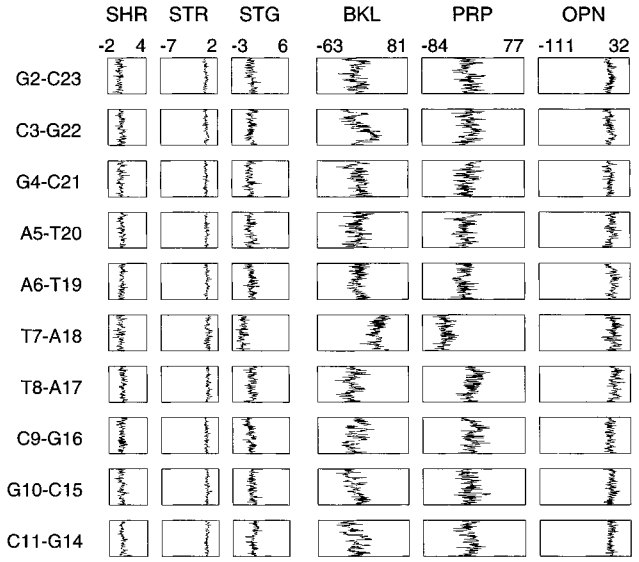

Figure 6. Intra base-pair parameters illustrating the geometry of base pairing in the lesioned dodecamer: shear (SHR), stretch (STR), stagger (STG), buckle (BKL), propeller twist (PRP), and opening (OPN). Time of the simulation increases from the bottom to the top of the window.

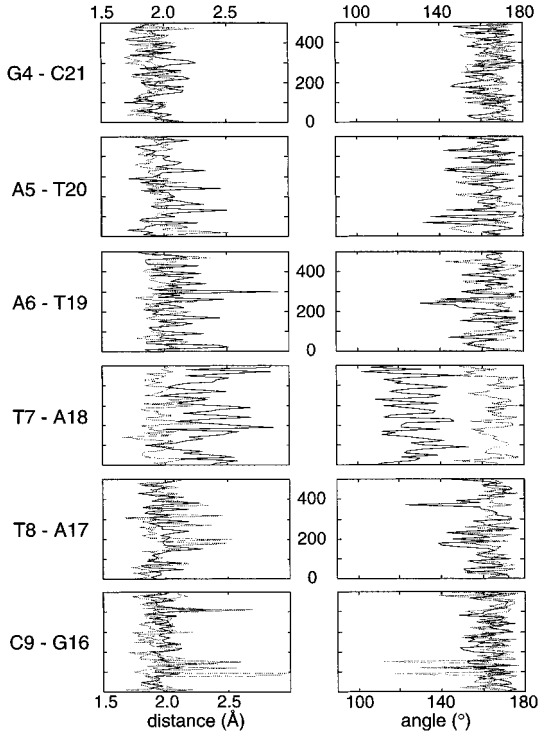

Figure 7. Lengths and angles of Watson−Crick hydrogen bonds for the six central base-pairs of the lesioned dodecamer. Time of the simulation increases from 0 to 500 ps from the bottom to the top of the window.

and thus it is closer to ^{2}E conformation characteristic of A-DNA. Similar conformational preference was postulated for the d(TpT) dinucleoside containing the dimer based on NMR measurement.[37]

Probably the major structural perturbation predicted by our calculations concerns base-pairing at the 5′ thymine of the dimer. We find one of the hydrogen bonds at this T:A base pair stretched to 2.5 Å with the hydrogen bond angle decreased to 120° due to significant buckling and propeller twist. This observation is consistent with NMR data obtained from imino protons spectra for a lesioned octamer where weakening (but not disruption) of the hydrogen bonds at both lesioned thymines was observed[14,18] but with more severe weakening at the 5′ thymine.[14] Interestingly, in the recently determined crystal structure of the complex formed between endonuclease V and dimer containing DNA, an adenine base was found rotated out of the helix.[10] This flipped-out adenine is complementary to the 5′ lesioned thymine for which our simulations predict severe weakening of Watson−Crick hydrogen bonds.

Perturbations in base-stacking interactions are also detected in our calculations. These perturbations are mainly in the form of tilt and roll angles and are observed between the two lesioned base pairs and to a smaller extent between the 5′ lesioned thymine and the adjacent A:T base pair. These distortions in tilt and roll are a direct effect of sterical restraints imposed by the cyclobutane linkage; formation of a cyclobutane ring simply disallows parallel stacked bases as normally seen in DNA. However, it should be emphasized that, except for small

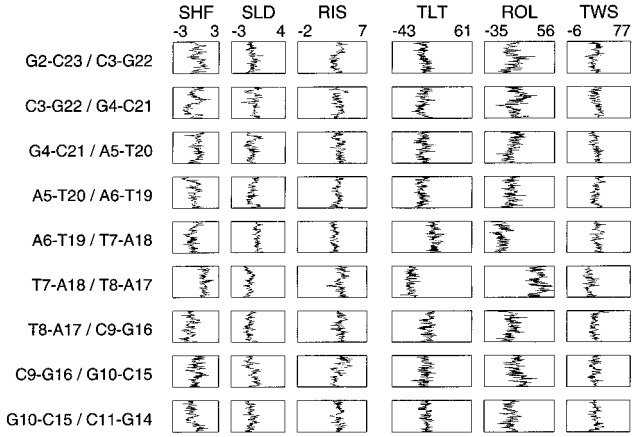

Figure 8. Inter base-pair parameters illustrate the geometry of base stacking in the lesioned dodecamer: shift (SHF), slide (SLD), rise (RIS), tilt (TLT), roll (ROL), and twist (TWS).

distortions observed near the dimer, base-pairing and base-stacking interactions are, in general, well preserved in the lesioned sequence. Similar conclusions about retained stacking and hydrogen bonding in dimer containing DNA were made based on thermodynamics characteristics evaluated from DNA melting behavior.[17,19] Some small unspecified distortions at the bases flanking the dimer on the 3′ side have been postulated[17,18] on the basis of NMR spectra. We do not see any substantial perturbations there as well as anywhere outside the dimer position.

Taylor et al. reported,[17] that all H(1′)-H(6)(pyrimidine)/H(8)-(purine) cross-peaks were observed in the 2D-NMR NOESY spectrum of the decamer d(CGTATTATGC)$_2$ containing a *cis,syn*-cyclobutane thymine dimer with the exception of H(1′)-(A4)-H(6)(T5), where T5 is the 5′ thymine of the dimer. A similar interruption was also noted for the dimer containing octamer d(GCGTTGCG)$_2$ 16 and decamer d(CGCATTACGC)$_2$ 13. Such an interruption in NOE connectivity is an indicator of extended interatomic distance, presumably longer than 5 Å. The only H(1′)-H(6)/H(8) distance in our simulation on d(CG-CAATTCGCG)$_2$ that exceeds 5 Å is A6/T7 (Table 1). Since T7 is the 5′ thymine of the dimer in our simulation, this result fully agrees with the NMR data even though the sequence context of the cyclobutane thymine dimer is somewhat different.

T4 endonuclease V interacts with the minor groove of DNA containing a thymine dimer.[10,38] This result raises the question of possible recognition factors in the DNA minor groove near a dimer site. Structures generated in the present simulation were analyzed from this point of view, but no peculiarities in the minor groove properties, such as width, depth or interphosphate distances, were found around the dimer site. The crystal structure of endo V complexed with dimer-containing DNA shows interactions between protein residues (Arg26 and Thr2) and C(2)═O(2) groups of both lesioned thymines.[10] Average distances between O(2) atoms of the neighboring thymines from the 300−500 ps time period of our simulation are 5.0 Å for the damaged thymines (T7 and T8) and 4.3 Å for the nondamaged (T19 and T20) thymines. In the native dodecamer, a value of 4.5 Å was found for both T7-T8 and T19-T20. Therefore, it seems likely that a different relative orientation of potential targets in the minor groove (e.g., O(2) atoms) at the dimer site could be one of the factors contributing to endonuclease V recognition specificity.

In earlier work (Miaskiewicz, Miller, and Osman, unpublished results), similar MD simulations were performed on the same oligonucleotides (native and damaged) as in the present work but using the older force-field of Weiner et al.[39] and with nonbonded interactions truncated at the cutoff distance of 11 Å. Interestingly, the pattern of local dimer-induced distortions found in the earlier work was very similar to those predicted by the present simulations. This indicates that local dimer-induced changes to DNA conformation are not very sensitive to the method used to treat long-range electrostatic interactions. These local deformations, which are the predominant effect of the lesion, depend primarily on the geometry of cyclobutane ring formation between neighboring thymines. It should be noted, however, that large differences in global structural characteristics were found between these two sets of calculations, i.e., with nonbonded cutoff and with PME method. For example, a very large mean curvature angle of about 80° was predicted for both native and damaged sequences in simulations with truncated electrostatic interactions.

Conclusions

Results of computer simulations on the DNA dodecamer d(CGCGAATTCGCG)$_2$ with and without a cyclobutane thymine dimer correlate very well with the available experimental data. These simulations give a picture of lesion-induced distortions localized almost exclusively at the dimer site which consist primarily of a substantial kink in the helical axis, rolled and tilted base pairs of the dimer, and weakened hydrogen bonding at the 5′ base pair of the lesion. No significant nonlocal distortions are found except for slight attenuation of kinks in the native dodecamer at the C3/G4 and C9/G10 steps. The net effect of the local dimer-induced kink and this attenuation of native kinks is an increase in the overall curvature angle by about 10°. Since pre-existing kinks in the native sequence are involved, the small effect of the dimer on global curvature found in this case may not be typical of the thymine dimer in other sequence contexts. The predominance of local distortions found in these simulations is consistent with results reported from NMR measurements on dimer containing oligonucleotides. In addition, the pattern of H(1′)-H(6)/H(8) intrastrand distances calculated from our trajectories agrees very well with observed NOE spectra in dimer containing oligonucleotides.

The main objective of our work on the thymine-dimer containing DNA is to provide insight into recognition of this lesion by enzymes such as, the most studied, T4 endonuclease V. Comparing our results with the published crystal structure of a DNA-endonuclease V complex[10] leads to an interesting hypothesis that the enzyme may not recognize any single particular structural/dynamical property at the dimer site but rather react on the whole pattern of small perturbations in DNA properties caused by presence of the dimer lesion. The sharp 60° kink toward the major groove observed in the complex formed between lesioned DNA and endonuclease V, already exists, although much smaller, at the dimer site in the lesioned sequence. The adenine base complementary to the 5′ lesioned thymine is totally rotated out of the helix in the crystal structure of the complex, and our simulations find severe weakening of Watson−Crick hydrogen bonds at this base-pair due to dimer formation. In addition, minor groove O(2) atoms of the lesioned thymines involved in contacts with endonuclease V in the complex have a different relative orientation in the lesioned T/T step than observed in undamaged T/T steps. All of these factors may not be specific for the dimer site when taken separately, however, their combination at the T/T step may provide enough specificity for high level of recognition by endonuclease V (and

(38) Iwai, S.; Maeda, M.; Shimada, Y.; Hori, N.; Murata, T.; Morioka, H.; Ohtsuka, E. *Biochemistry* **1994**, *33*, 5581−5588.

(39) Weiner, S. J.; Kollman, P. A.; Nguyen, D. T.; Case, D. A. *J. Comput. Chem.* **1986**, *7*, 230−252.

other repair enzymes). It is also possible that the recognition mechanism depends, at least partially, on other factors such as perturbation in the pattern of hydration or counterions distribution around the dimer site.[40] We are actively pursuing a detailed analysis of the behavior of hydrating water and counterions in our simulations that will be presented in a separate publication.

Calculations are in progress for thymine dimers in other DNA oligonucleotides for detailed comparison with NMR data from our own laboratory. These works should add to our understanding of the pattern of DNA structural and dynamical distortions caused by the thymine dimer lesion, their dependence on sequence context, and their relevance to lesion recognition by repair enzymes.

(40) Osman, R.; Luo, N.; Miaskiewicz, K.; Miller, J. *Radiation damage in DNA: Structure/function relationships at early times;* Fuciarelli, A. F., Zimbrick, J. D., Eds.; Batelle Press: Columbus, OH, 1995; pp 323−330.

Acknowledgment. The authors gratefully acknowledge assistance by Dr. Osmar Norberto de Souza in calculations of DNA curvature. This work was supported by the Office of Health and Environmental Research (OHER) of the U.S. Department of Energy under contract DE-AC06-76RLO 1830, DOE Grant DE-FG02-88ER60675, and the Public Health Service Grant CA63317.

JA9611304